METALS AND MATERIALS International, Vol. 9, No. 2 (2003), pp. 207~213

Characterization of the Chemical Conversion Films that Form on Mg-Al Alloy in Colloidal Silica Solution

Seong-Jong Kim[1,*], Ying Zhou[1], Ryoichi Ichino[1], Masazumi Okido[1], and Shoji Tanikawa[2]

[1] Graduate School of Engineering, Nagoya University
Furo-cho, Chikusa-ku, Nagoya, 464-8603, Japan
[2] Nakanihon Die Casting Co., Ltd.
Kinzoku Tanchi 188, Kakamihara, 504-0957, Japan

Chemical conversion treatment of Mg-Al alloy (AZ91) using colloidal silica as an alternative to chromate conversion was investigated as a function of solution pH, temperature, solution conditions, and treatment time. The solution used for the colloidal silica coating consisted of colloidal silica, titanium sulfate, and cobalt ions to maintain good anti-corrosion and adhesion properties. Adding $CoSO_4$ to the colloidal silica solution enhanced the adhesion force between the silica film and magnesium substrate. The optimum conditions for the chemical conversion treatment solution were pH 2, 90-sec treatment, and 25 °C.

Keywords : chemical conversion treatment, Mg-Al alloy, colloidal silica coating, corrosion resistance

1. INTRODUCTION

Magnesium must be surface treated to prevent corrosion because it is very active, electrochemically. Many surface treatments prevent the corrosion of magnesium and Mg-Al alloys, including chromate chemical conversion (CCC) [1-5], anodizing [6,7], painting, electroplating, etc. CCC films are still one of the most efficient surface treatments for Mg alloys and galvanized steel. CCC films have high anti-corrosion and anti-wear properties. However, chromate compounds are very toxic and carcinogenic [8]. Therefore, an alternative surface treatment for CCC is needed. The anti-corrosion properties, structure, and mechanism of chemical conversion coating formation on die-cast magnesium material (AZ91D) have been studied in various papers [7,9].

This study investigated chemical conversion treatment of Mg-Al alloy (AZ 91) using colloidal silica as the surface treatment, focusing on the effects of solution pH, temperature, solution condition, and treatment time.

2. EXPERIMENTAL PROCEDURE

AZ91 (Al 9 mass%, Zn 1 mass%) was mounted with epoxy resin, except for an exposed 1 cm^2 area, and polished with No. 2000 emery paper. The specimens were carefully degreased with acetone and water. Then, acid activation was executed in 2 mass% HNO_3 at 298 K for 5 sec. The conversion solution contains 200 mM colloidal silica (Nissan Chemical Industries, Ltd., Snowed) with 10-20 nm SiO_2 particles, 4.2 mM $Ti(SO_4)_2$, 1.8 mM $CoSO_4$, and 4.2 mM $C_2H_4(COOH)_2$. The solution pH was adjusted to 2 with HNO_3. Each specimen was rinsed with water after activation. The chemical conversion films formed on the specimens were dried at 353 K for 5 min.

The electrochemical system consisted of a Pt coil as a counter electrode, and an Ag/AgCl sat. KCl reference electrode. The anodic polarization curve was measured to characterize the corrosion properties of the chemical conversion treatment film using a potentiostat with a scan rate of 1 mV/s in 0.1 M NaCl and 0.1 M Na_2SO_4 solution at 298 K. In addition, the salt spray test (SST) was carried out at a spray rate of 1.5 ± 0.5 ml/(hr · 80 cm^2) using 50 ± 5 g/L NaCl at 35 ± 1 °C. The surface of the coated film was observed by optical and scanning electron microscopy (SEM), and analyzed by energy dispersive spectroscopy (EDS) and Fourier-transform-IR spectroscopy (FT-IR).

3. RESULTS AND DISCUSSION

The influence of solution condition, pH, temperature, and treatment time on the anti-corrosion properties with chemical conversion treatment was investigated. Using the conditions for activation only, no film was observed by SEM. Abbreviations S, C, K and T mean colloidal silica, $CoSO_4$, $C_2H_4(COOH)_2$, and $Ti(SO_4)_2$. More cracks were observed with (b)-(e) solution, than with (f) solution. It was suggested

---

*Corresponding author: kmue43aksj@hanmail.net

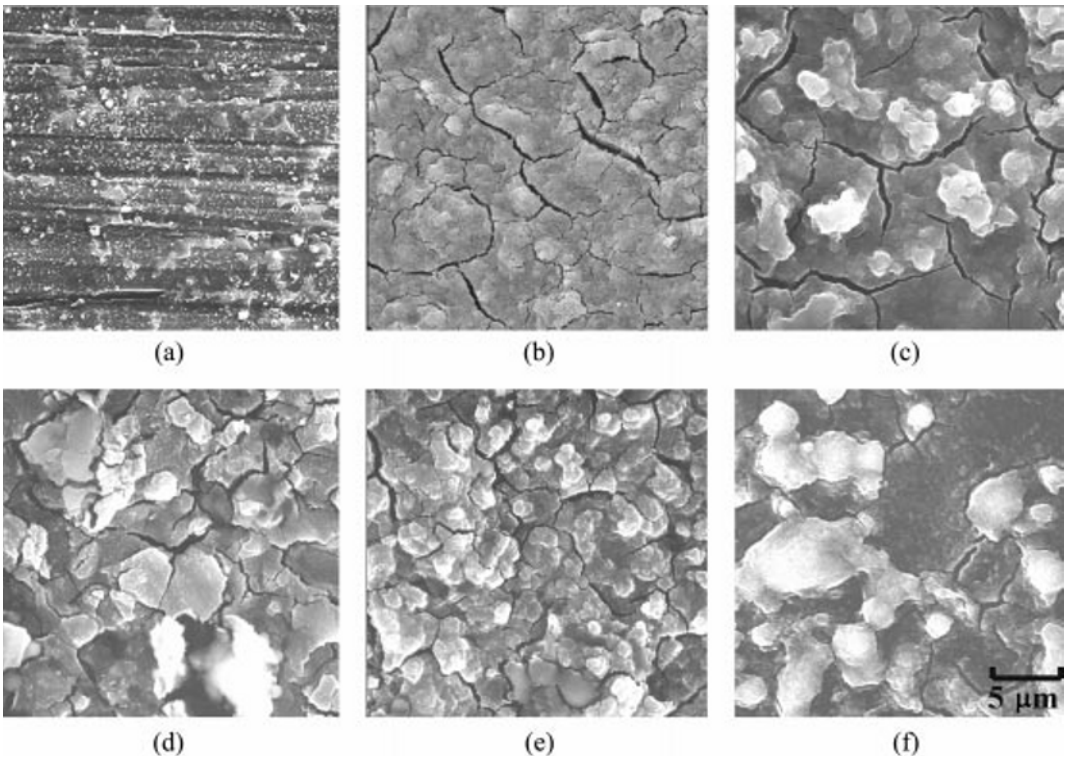

Fig. 1. Surface morphology after chemical conversion treatment as a function of solution condition: (a) Only activation; (b) C+K+T; (c) S+K+T; (d) S+C+K; (e) S+C+T; and (f) S+C+K+T. (S: Colloidal Silica, C: $CoSO_4$, K: $C_2H_4(COOH)_2$, T: $Ti(SO_4)_2$).

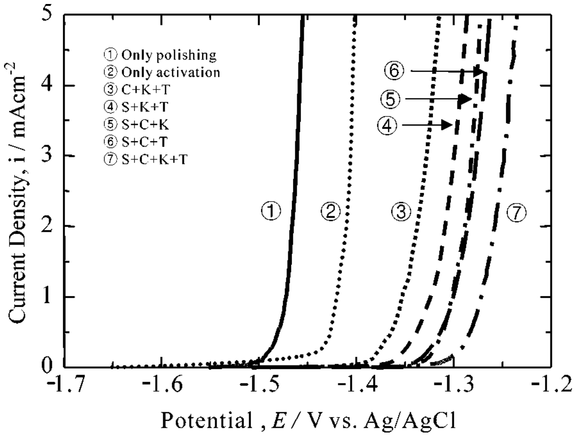

Fig. 2. Comparison of anodic polarization curves after chemical conversion treatment as a function of solution condition. The anodic polarization experiment carried out at 25 °C, pH 2 in 0.1 M NaCl and 0.1 M Na_2SO_4.

that the cracks form during drying at 80 °C for 5 min after chemical conversion treatment (Fig. 1).

Fig. 2 compares the anodic polarization curves after chemical conversion treatment as a function of solution condition. The anodic polarization experiment was carried out at 25 °C, pH 2, in 0.1 M NaCl and 0.1 M Na_2SO_4. The anti-corrosion properties with various chemical conversion treatments were better than with polishing or activation alone. Potential at which the current density reached 1 mA/cm^2 compared at various solution conditions. Potentials in only polishing, only activation, C+K+T, S+K+T, S+C+K, S+C+T and S+C+K+T were −1.47, −1.42, −1.3505, −1.325, −1.3, −1.3 and 1.273 V, respectively. Therefore, potential in S+C+K+T was more noble than the other solution conditions. The anti-corrosion properties of specimens that were chemical conversion treated in solution without colloidal silica (S) were inferior to the other solution conditions. The solution containing colloidal silica (S), $CoSO_4$ (C), $C_2H_4(COOH)_2$ (K), and $Ti(SO_4)_2$ (T) conferred excellent anti-corrosion properties compared with the other conditions. As Figs. 1 and 2 show, the essential elements required to form a film during chemical conversion treatment were colloidal silica, $CoSO_4$, $C_2H_4(COOH)_2$, and $Ti(SO_4)_2$.

Fig. 3 shows the results of peeling tests of films formed with and without $CoSO_4$. The test method was carried out according to JIS A 5422. Cobalt ions markedly reduced the size of the grains in the silica films and improved the adhesion of the silica films to the Mg-Al alloy. Cracks on the film surface are generated by surface tension as water evaporates with drying. As the adhesion between the Mg-Al alloy substrate and film is enhanced, the contractile force acting on the film is dispersed, and the grains become finer. When the magnesium is dissolved, hydrogen gas is generated on the

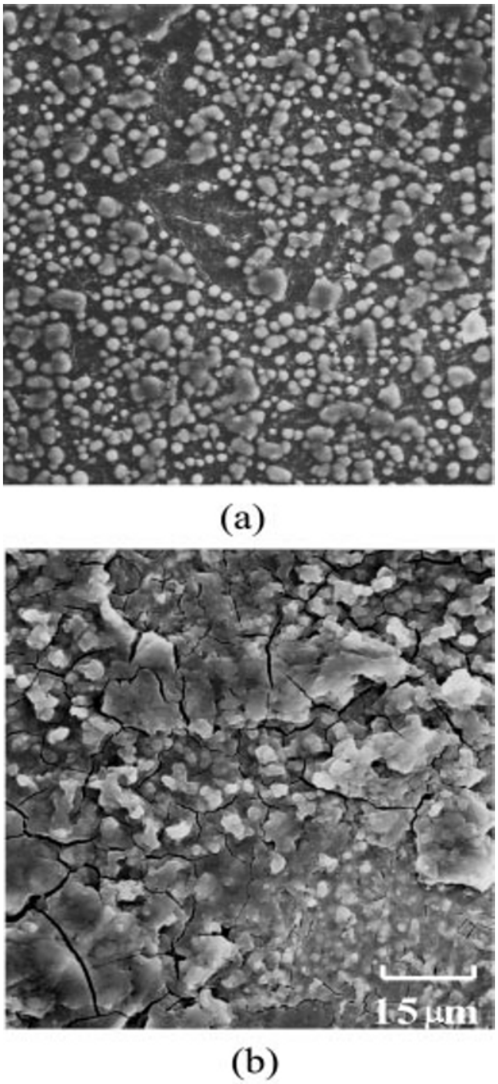
(a)

(b)

Fig. 3. Results of the peeling test after chemical conversion treatment with and without $CoSO_4$ in the standard solution: (a) S+C+K+T (Standard solution) and (b) S+K+T.

Mg-Al alloy substrate. It was postulated that replacing some of the magnesium with cobalt ions from $CoSO_4$ increased the interface adhesion force. The film thickness at cross section observation was about 3 μm.

The effect of added $Ti(SO_4)_2$ on the zeta-potential of the colloidal silica particles and silica film formation is evaluated in Fig. 4. The surface potential of silica particles changes with the concentrations of H^+ and OH^- ions. At low pH, H^+ is attracted to the OH^- hydrated to the Si. When the charge on the silica surface is balanced exactly, this is the point of zero charge (PZC) of the hydrogen ion concentration [10].

The zeta-potential in solutions without $Ti(SO_4)_2$ averaged ca. –30 mV, while the zeta-potential in solutions with $Ti(SO_4)_2$ was ca. +20 mV. $Ti(SO_4)_2$ shifted the surface potential of the silica particles so that it became positive. This change in the surface potential is also utilized to disperse TiO_2 paint pigments uniformly, by adding silica or alumina, which change the surface potential of the TiO_2 particles in paints [11,12].

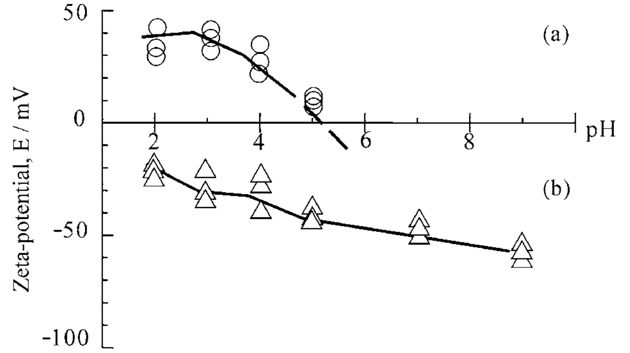

Fig. 4. Effect of conversion solution pH on the zeta-potential of silica particles in conversion solutions of colloidal silica solution (a) with and (b) without $Ti(SO_4)_2$.

Since the local solution pH near the specimen increased with magnesium dissolution, and hydrogen evolution occurred during chemical conversion, the effect of solution pH was examined on the zeta-potential of silica particles in colloidal silica solution with and without $Ti(SO_4)_2$. The pH was adjusted with HNO_3 and NH_3. Without $Ti(SO_4)_2$, the zeta-potential became more negative as pH increased. Conversely, the surface charge changed from positive to negative at pH 5 (*i.e.*, this is the PZC) in the solution with $Ti(SO_4)_2$. The white turbidity phenomenon observed in high pH regions became more pronounced with the addition of $Ti(SO_4)_2$. Gelation did not occur readily in silica particles with a negative surface charge, but gelation and film formation did occur readily after the silica particles passed the PZC. These results suggest that a film forms on the surface of Mg-Al alloy as a result of the change in the zeta-potential of the silica particles. We attempted to measure the change in the zeta-potential with increasing pH, but could not, due to the turbidity that developed.

Fig. 5 compares anodic polarization curves as a function of treatment time during chemical conversion treatment at pH 2 and 25 °C. At comparison of potential at which the current density reached 1 mA/cm^2 as a function of chemical conversion treatment time, potential in 90-sec treatment time was –1.275 V, and has the best corrosion resistance. The optimum treatment time was 90 sec, and the anti-corrosion properties decreased with increasing time above 90 sec. Chemical conversion treatment time was not proportional to the corrosion resistance. With increasing treatment time, the grain size divided by cracks in the film surface increased. Specimen weight with activation only decreased by about 0.2 mg/cm^2, while the weight after a 90-sec treatment increased by ca. 0.1 mg/cm^2 with formation of a conversion film. With a

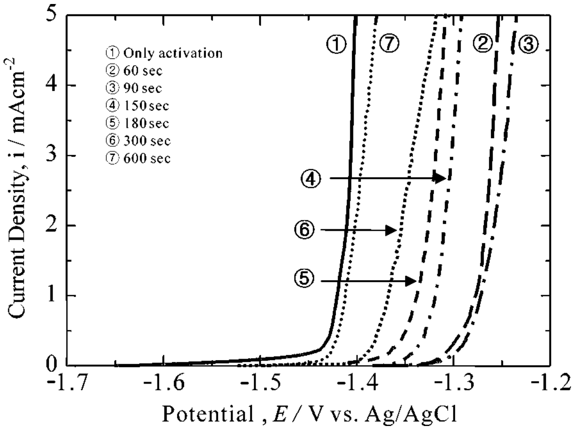

Fig. 5. Comparison of anodic polarization curves as a function of chemical conversion treatment time.

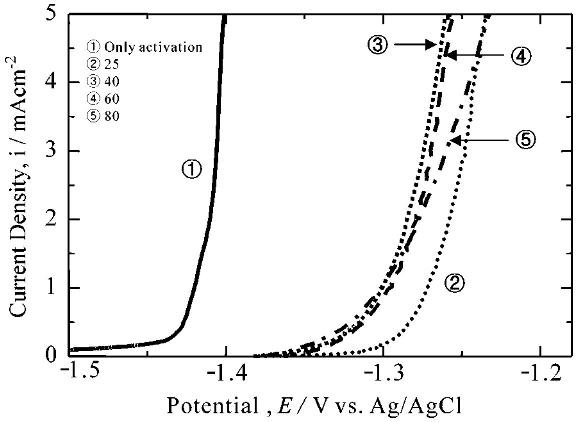

Fig. 6. Comparison of anodic polarization curves as a function of chemical conversion solution temperature.

150-sec treatment, the weight increased about 0.04 mg/cm^2, while at treatments exceeding 300 sec, it increased by ca. 0.18 mg/cm^2. It is considered therefore that chemical conversion treatment time is not proportional to the weight variation.

Fig. 6 shows the anodic polarization curves as a function of solution temperature at pH 2 in the standard additive solution. With time, the color of the film changed from white to gray, and the surface became rough. Moreover, the anti-corrosion properties with chemical conversion at various temperatures were better than with activation alone. No large differences in the anti-corrosion properties were found with treatments at temperatures of 40-80 °C, and the best anti-corrosion properties were with treatment at 25 °C.

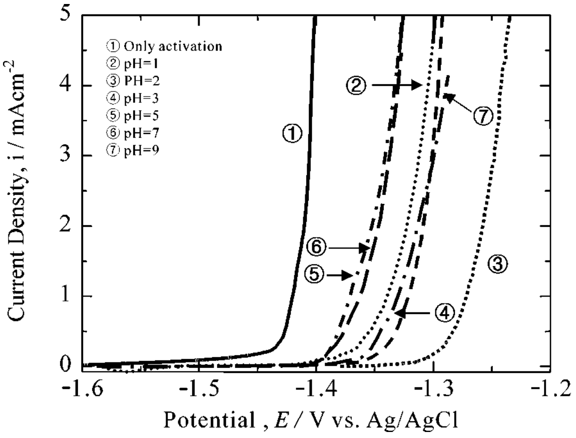

Fig. 7. Comparison of anodic polarization curves as a function of pH during chemical conversion treatment.

Fig. 7 compares the anodic polarization curves as a function of pH during chemical conversion treatment. The solution at pH 2 contained 200 mM colloidal silica, 4.2 mM $Ti(SO_4)_2$, 1.8 mM $CoSO_4$, and 4.2 mM $C_2H_4(COOH)_2$. The pH was adjusted to 1-9 with HNO_3 or NH_4OH. At a pH above 5, the white turbidity phenomenon was detected. Potentials at which the current density reached 1 mA/cm^2 in pH 1, 2, 3, 5, 7 and 9 were −1.343, −1.273, −1.33, −1.375, −1.365 and −1.323 V, respectively. The anti-corrosion properties with treatment at various pHs were better than with activation alone.

This study of chemical conversion treatment focused on the effects of pH, temperature, and treatment time. The optimum chemical conversion treatment conditions used solutions at pH 2 and 25 °C, with 90-sec treatment. We call these optimum conditions the standard solution conditions. We examined the existence of silica films in colloidal silica solution adjusted to pH 2 using HNO_3, HCl, or H_2SO_4. No films formed in HCl or H_2SO_4. It was suggested that the chemical conversion films only form in HNO_3 because the oxidation force of HNO_3 is powerful. It is thought that Si-O-Mg bonds are generated at the interface between the film and the Mg-Al alloy [13]. According to Johnson *et al.*, when zinc is immersed in HNO_3, the HNO_3 dissolves the zinc surface, generating very active zinc particles at the dissolved zinc surface [14-16]. We postulate that similar changes occur with Mg-Al alloy.

EDS did not show a large difference in magnesium with activation only, and no oxygen was detected in the substrate or film. Large amounts of silicon and oxygen were detected in chemical conversion films formed in the standard solution, while there was less magnesium in the Mg substrate. The film was about 2-3 μm thick (Fig. 8).

Fig. 9 shows an SEM image of the surface morphology after chemical conversion treatment in standard solution and standard solution containing 1.0 g/L polyvinyl acid (PVA), 1.0 g/L polyacrylic acid (PAA), and 1.0 g/L polyaspartic acid (PAsp), which is known as 3P solution. 3P solution is used to improve the gelation of the colloidal silica and the anti-corrosion properties. PVA promotes the gelation of colloidal silica via hydrogen bonding between hydroxide ions on the surface of the silica particles and PVA [17]. The chemical conversion film formed in standard solution was

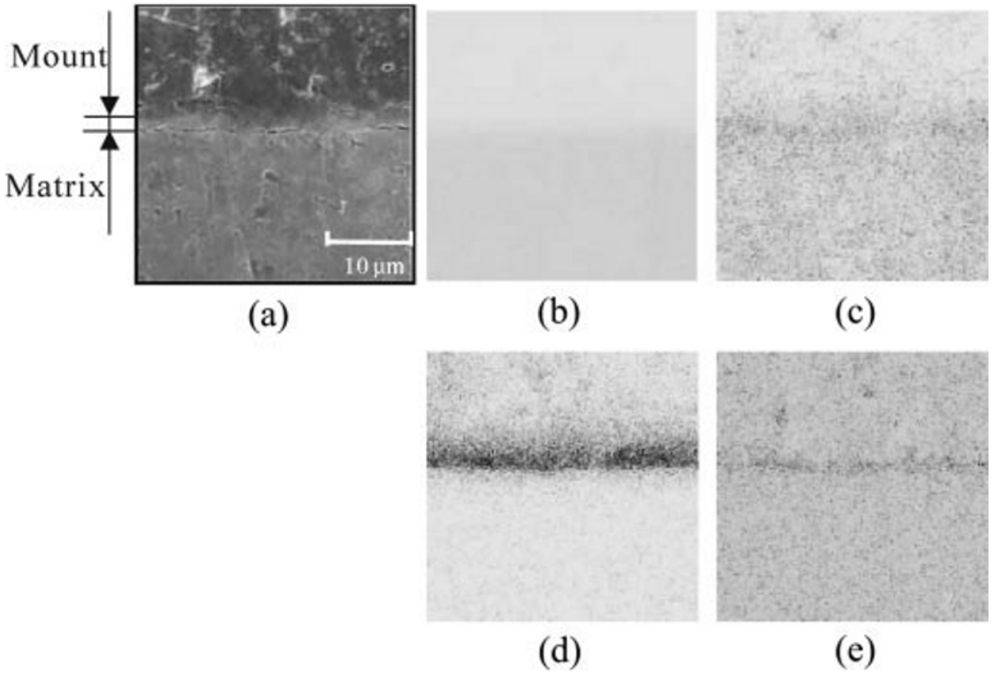

Fig. 8. SEM photographs and results of EDS analysis after chemical conversion treatment in standard solution: (a) cross section photography; (b) Mg; (c) Al; (d) Si; and (e) O.

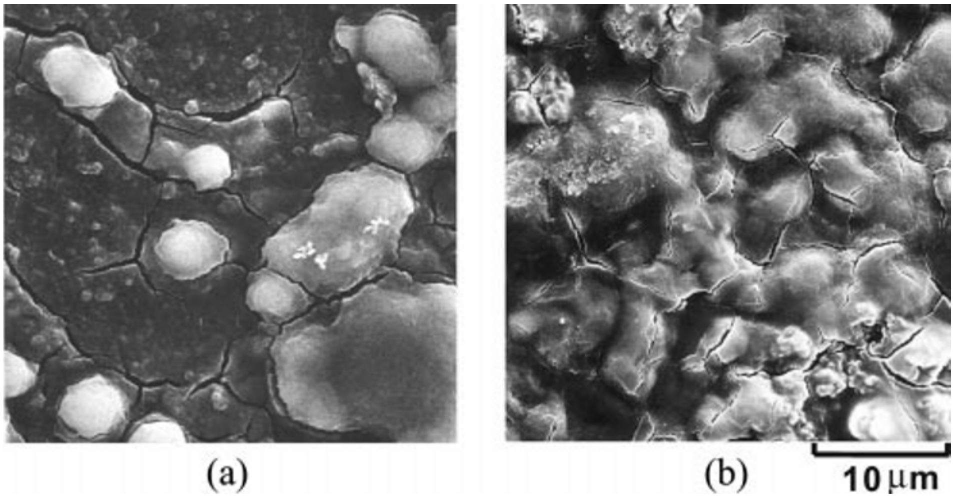

Fig. 9. SEM image of the surface morphology after chemical conversion treatment using standard solution with and without 3P (PAsp, PVA, PAA): (a) silica conversion solution and (b) silica conversion solution + (PAsp, PVA, PAA).

white, shiny metal was seen, and many cracks were observed. These cracks in the film surface were shallower and finer in standard solution containing 3P.

Fig. 10 compares the FT-IR spectra of films obtained with chemical conversion solution with and without 3P. Peaks due to Si-O-Si, C-O-Si, CH_2, -OH, and C-H are seen in both films, but the Si-O-Si, C-O-Si, and -OH peaks are stronger with the chemical conversion solution containing 3P. Especially, the C-O-Si peak is remarkably high.

Fig. 11 compares the anodic polarization curves with polishing alone and with chemical conversion in various solutions. Potentials at which the current density reached 1 mA/cm^2 in without and with 3P were −1.275 and −1.259 V. The anti-corrosion properties in chemical conversion treated were much better than that in polishing only, remarkably. In addition, the film with solution containing 3P was much better than that with standard chemical conversion solution. Nevertheless, the results of the salt spray test for 48 hr were

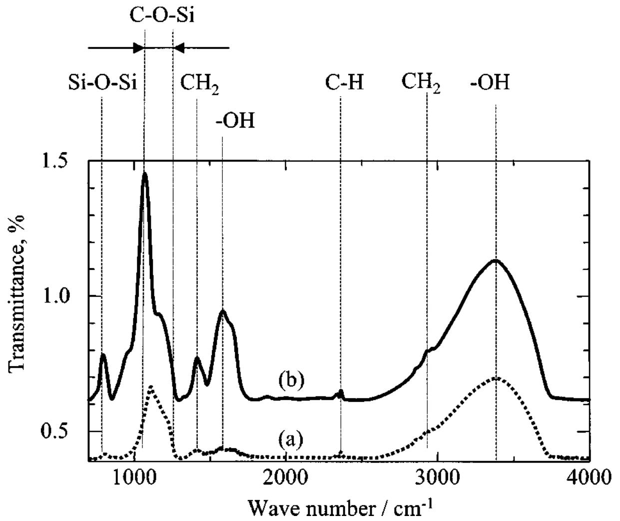

Fig. 10. FT-IR spectrum of the film formed from chemical conversion solution (a) without and (b) with 3P.

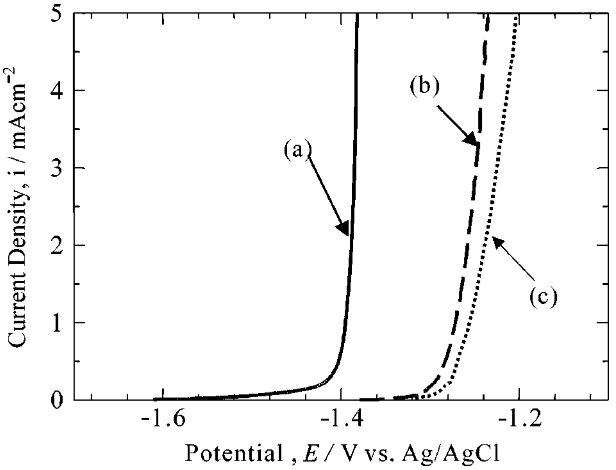

Fig. 11. Comparison of the anodic polarization curves after chemical conversion treatment as a function of solution condition: (a) polishing only; (b) chemical conversion solution; and (c) chemical conversion solution with 3P.

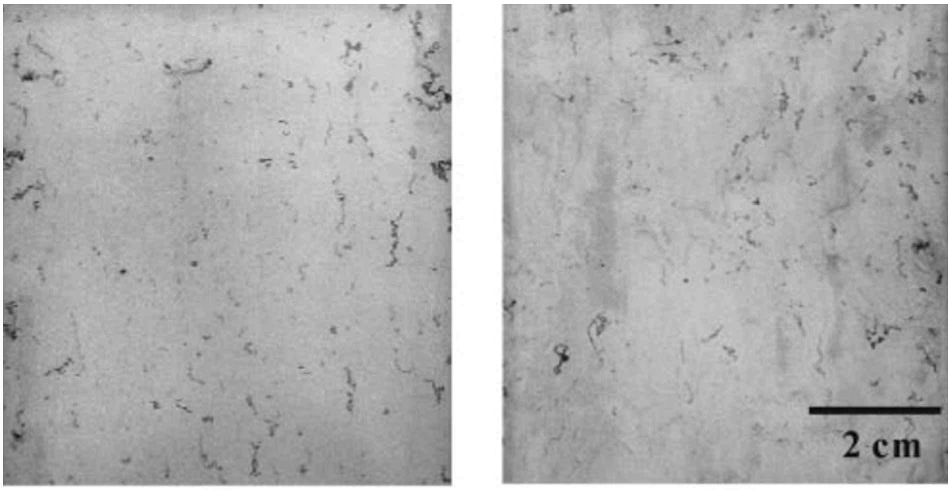

(a) (b)

Fig. 12. Comparison of photography after salt spray test for 48 hr in (a) chemical conversion solution, (b) chemical conversion solution with 3 P.

similar for silica conversion solution with and without 3P (Fig. 12).

4. CONCLUSIONS

The essential elements required to form a film during chemical conversion treatment were colloidal silica, $CoSO_4$, $C_2H_4(COOH)_2$, and $Ti(SO_4)_2$. Adding $CoSO_4$ to the colloidal silica solution enhanced the adhesion between the silica film and the magnesium substrate. The optimum conditions were pH 2, treatment time 90 sec, and 25 °C. Chemical conversion treatment time is not proportional to the anti-corrosion property and weight variation. If the silica particles reach the point of zero change, gelation and formation of a film are readily accomplished. The anti-corrosion properties of films formed in chemical conversion solution containing PVA, PAA, and PAsp were better than those of films formed in standard chemical conversion solution.

ACKNOWLEDGMENT

The authors would like to acknowledge support for this research from the Japan Society for the Promotion of Science.

REFERENCES

1. R. G. Buchheit, R. P. Grant, P. F. Hlava, B. Mckenzie, and

G. I. Zender, *J. Electrochem. Soc.* **144**, 2621 (1997).

2. Z. A. Foroulis and M. J. Thubrikar, *J. Electrochem. Soc.* **122**, 1296 (1975).
3. J. A. Richardson and G. C. Wood, *J. Electrochem. Soc.* **120**, 193 (1973).
4. H. Bohni and H. H. Uhlig, *J. Electrochem. Soc.* **116**, 906 (1969).
5. G. O. Ilevbare and J. R. Scully, *J. Electrochem. Soc*. **148**, B196 (2001).
6. S.-J. Kim, Y. Mizutani, M. Okido, R. Ichino, S. Tanikawa, and S. Hasegawa, *Mater. Trans*. (be submitted).
7. Y. Mizutani, S. J. Kim, R. Ichino, and M. Okido, *The 6th ASFF, AEPSE 2001, 5th APIC, and 4th JKSPTFT: Anodizing Mg Alloys on Alkaline Solutions, Frontiers of Surface Engineering 2001 Conf. and Exhibition*, p. 178, The Surf. Finishing Soc. Jpn, Nagoya, Japan (2001).
8. H. Umehara, M. Takaya, and Y. Kojima, *J. Jpn. Inst. Light Met*. **50**, 109 (2000).
9. S. Ono, M. Saito, M. Horigochi, K. Terashima, K. Matsusaka, A. Shida, T. Osaka, and N. Masuko, *The Surf. Finishing Soc. Jpn*. **47**, 263 (1996).
10. K. Masatosi and T. Kazuo, *Interfacial Chemistry*, p. 135, Maruzen (2001).
11. K. Manabu, *Oxidation Titanium*, p. 255, Gihodo Publ. Co. (2000).
12. T. Hongxia, *Appl. Cataly. B* **30**, 277 (2001).
13. S. Saihu, *Science of the Sol-Gel Method*, p. 88, Magune-shouhusha (1988).
14. J. W. Johnson and W. J. James, *Corros. Sci.* **11**, 153 (1971).
15. J. W. Johnson and W. J. James, *Corrosion* **23**, 15 (1967).
16. D. C. Stiles and E. O. Edney, *Corrosion* **45**, 896 (1989).
17. Y. Liu, W. Ren, L. Zhang and X. Yao, *Thin Solid Films* **353**, 124 (1999).